The Astrophysical Journal Letters, 899:L26 (6pp), 2020 August 20 https://doi.org/10.3847/2041-8213/abacc9

Color Gradients along the Quiescent Galaxy Sequence: Clues to Quenching and Structural Growth

Katherine A. Suess[1], Mariska Kriek[1], Sedona H. Price[2], and Guillermo Barro[3]
[1] Astronomy Department, University of California, Berkeley, CA 94720, USA; suess@berkeley.edu
[2] Max-Planck-Institut für extraterrestrische Physik, Postfach 1312, Garching, D-85741, Germany
[3] Department of Physics, University of the Pacific, 3601 Pacific Avenue, Stockton, CA 95211, USA
Received 2020 June 19; revised 2020 July 31; accepted 2020 August 6; published 2020 August 19

Abstract

This Letter examines how the sizes, structures, and color gradients of galaxies change along the quiescent sequence. Our sample consists of ∼400 quiescent galaxies at $1.0 \leqslant z \leqslant 2.5$ and $10.1 \leqslant \log M_*/M_\odot \leqslant 11.6$ in three CANDELS fields. We exploit deep multi-band Hubble Space Telescope imaging to derive accurate mass profiles and color gradients, then use an empirical calibration from rest-frame *UVJ* colors to estimate galaxy ages. We find that—contrary to previous results—the youngest quiescent galaxies are *not* significantly smaller than older quiescent galaxies at fixed stellar mass. These "post-starburst" galaxies only appear smaller in half-light radii because they have systematically flatter color gradients. The strength of color gradients in quiescent galaxies is a clear function of age, with older galaxies exhibiting stronger negative color gradients (i.e., redder centers). Furthermore, we find that the central mass surface density Σ_1 is independent of age at fixed stellar mass, and only weakly depends on redshift. This finding implies that the central mass profiles of quiescent galaxies do not significantly change with age; however, we find that older quiescent galaxies have additional mass at large radii. Our results support the idea that building a massive core is a necessary requirement for quenching beyond $z = 1$, and indicate that post-starburst galaxies are the result of a rapid quenching process that requires structural change. Furthermore, our observed color gradient and mass profile evolution supports a scenario where quiescent galaxies grow inside-out via minor mergers.

Unified Astronomy Thesaurus concepts: Galaxy evolution (594); Galaxy quenching (2040); Galaxy formation (595); Galaxy structure (622)

1. Introduction

Building a dense central core appears to be a prerequisite for forming massive quiescent galaxies (e.g., Cheung et al. 2012; Fang et al. 2013; van Dokkum et al. 2014; Tacchella et al. 2015; Mosleh et al. 2017; Whitaker et al. 2017). Galaxies cease forming stars after reaching a threshold in central mass surface density Σ_1 (e.g., Barro et al. 2016; Lee et al. 2018; Woo & Ellison 2019) or central velocity dispersion (e.g., van Dokkum et al. 2015). At the same time, the observed variations in the properties of quiescent galaxies across cosmic time indicate that galaxies continue to evolve after quenching their star formation, likely due to growth via dry minor mergers (e.g., Bezanson et al. 2009; Hopkins et al. 2009; Naab et al. 2009; van de Sande et al. 2013; Greene et al. 2015). Despite a broad consensus in the literature, there are still major uncertainties with this view of quiescent galaxy formation and evolution: the exact physics of the quenching process is still unknown, and the amount of growth that quiescent galaxies experience after quenching is debated (e.g., Carollo et al. 2013; Poggianti et al. 2013; Lilly & Carollo 2016).

The sizes and structures of young quiescent galaxies could hold clues to the physical processes responsible for quenching. Furthermore, comparing the sizes and structures of young and old quiescent galaxies could provide insight into how galaxies grow after quenching. While quiescent galaxies at fixed mass are smaller than their star-forming progenitors (e.g., van der Wel et al. 2014), the youngest quiescent galaxies—or "post-starburst" galaxies—appear to be even smaller than their older counterparts (Whitaker et al. 2012; Belli et al. 2015, 2019; Yano et al. 2016; Almaini et al. 2017; Maltby et al. 2018; Wu et al. 2020). These observations imply that sizes do not simply evolve passively: galaxies appear to shrink when they quench, then grow again as they age. In addition to their observed small sizes, post-starburst galaxies are incredibly compact, with high stellar mass densities (Almaini et al. 2017; Maltby et al. 2018). This may indicate that they reached a quenching density threshold after a rapid core-building process (or "compaction," e.g., Dekel & Burkert 2014; Zolotov et al. 2015; Tacchella et al. 2016).

These results are primarily based on studies of the light profiles of galaxies along the quiescent sequence. However, radial color gradients in galaxies are both a potential bias—they cause half-light and half-mass radii to differ, e.g., Suess et al. (2019a)—and a source of additional information, because color gradients represent radial variations in the underlying stellar populations of a galaxy. Studying the evolution of color gradients along the quiescent sequence, from post-starburst to old quiescent galaxies, is thus an additional method for probing the physical mechanisms responsible for galaxy growth and quenching. In this Letter, we present the half-mass radii, color gradients, and central mass surface densities of quiescent galaxies as a function of age.

We assume a cosmology of $\Omega_m = 0.3$, $\Omega_\Lambda = 0.7$, and $h = 0.7$, and a Chabrier (2003) initial mass function.

2. Sample and Methods

In this study we use the Suess et al. (2019a) catalog of color gradients and half-mass radii of galaxies at $1.0 \leqslant z \leqslant 2.5$ in three CANDELS fields (Grogin et al. 2011; Koekemoer et al. 2011). These measurements were made by fitting spatially

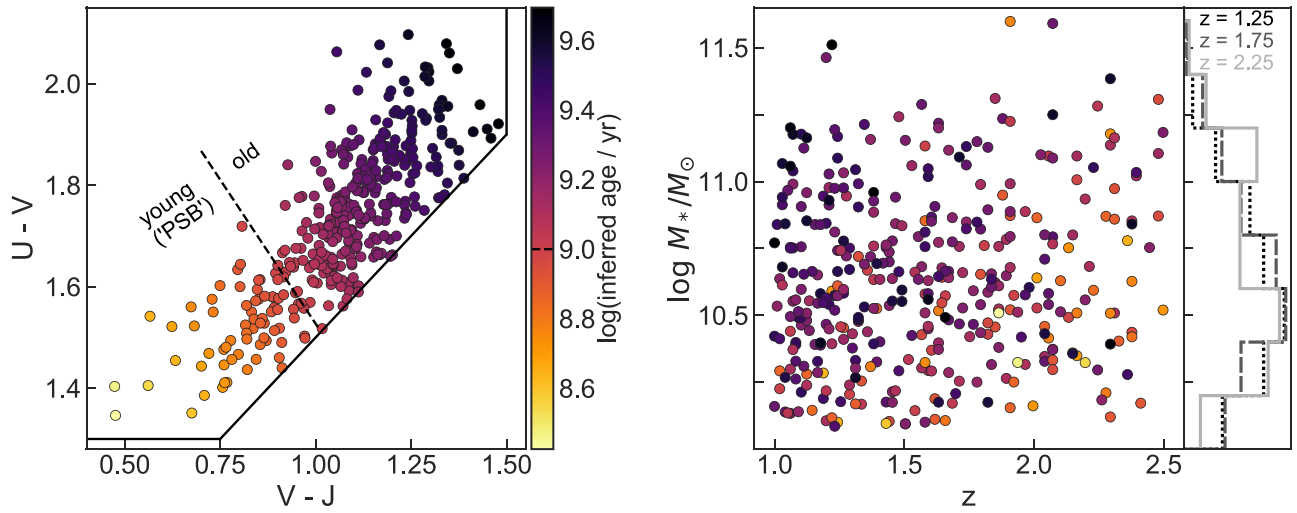

Figure 1. *UVJ* diagram (left panel) and stellar mass as a function of redshift (right panel) for our quiescent galaxy sample. Each galaxy is colored by its inferred stellar age using the Belli et al. (2019) mapping from *UVJ* colors to ages. Histograms show the normalized distribution of stellar masses in the three redshift bins used in this work. We only include quiescent galaxies with $M_* > 10^{10.1} M_\odot$, where our sample is complete.

resolved spectral energy distributions (SEDs) to find an observed-frame mass-to-light ratio (M/L) gradient. Then, a forward modeling technique was used to account for the point-spread function and recover intrinsic M/L gradients and half-mass radii.

We select 385 quiescent galaxies from the Suess et al. (2019a) catalog using the Whitaker et al. (2012) definition for quiescence based on rest-frame *UVJ* colors. We only include galaxies with $M_* > 10^{10.1} M_\odot$, where our sample is mass-complete (Suess et al. 2019a). Our sample lies in the overlap of the CANDELS and ZFOURGE (Straatman et al. 2016) fields, allowing for accurate measurements of both mass profiles and rest-frame SEDs.

Our study also requires estimates of the age of each galaxy. We use the Belli et al. (2019) prescription, who use deep continuum spectroscopy of quiescent galaxies to calibrate a mapping between *UVJ* colors and average stellar ages. Systematic uncertainties on ages calculated using this method are $\sim$0.13 dex. We refer to the youngest quiescent galaxies as "post-starburst" galaxies; however, see e.g., Wild et al. (2020) for a discussion of spectroscopically versus photometrically selected post-starburst galaxies.

Figure 1 shows our sample in *UVJ* and mass-redshift space. Each galaxy is colored by its inferred stellar age using the Belli et al. (2019) technique.

3. Sizes and Color Gradients of Quiescent Galaxies as a Function of Age

We begin by examining the size–mass relation for galaxies along the quiescent sequence. The left panel of Figure 2 shows the size–mass relation using half-light radii at rest-frame 5000 Å (van der Wel et al. 2014). Large points show the median sizes of both old (inferred age >1 Gyr) and young or "post-starburst" (inferred age <1 Gyr) quiescent galaxies in bins of stellar mass. We recover the result that post-starburst galaxies have smaller half-light radii than older quiescent galaxies (Whitaker et al. 2012; Belli et al. 2015, 2019; Yano et al. 2016; Almaini et al. 2017; Maltby et al. 2018; Wu et al. 2018). As noted by Almaini et al. (2017), this size difference is especially apparent at $M_* > 10^{10.5} M_\odot$.

The right panel of Figure 2 shows the size–mass relation for the same sample, this time using half-*mass* radii. The stark difference between the sizes of young and old quiescent galaxies disappears. While young quiescent galaxies have median half-light radii 0.3 dex smaller than their older counterparts, the difference in their median half-mass radii is only $\lesssim$0.1 dex.

We note that the large difference in the half-light radii of young and old quiescent galaxies is partially a redshift effect: the post-starburst galaxies in our sample have a slightly higher median redshift, and thus smaller half-light radii. However, our general result holds in narrow redshift slices: post-starburst galaxies have smaller half-light radii than older quiescent galaxies, but their half-mass radii are essentially consistent.

The fact that the difference between young and old quiescent galaxy sizes significantly shrinks when using half-mass radii is an indication that the two populations have systematically different color gradients. In Figure 3, we show color gradient strength versus galaxy age. Following Suess et al. (2019a, 2019b), we quantify color gradient strength by the log ratio of the half-mass and half-light radii of the galaxy: negative (positive) values indicate that the center of the galaxy is redder (bluer) than the outskirts. We show three redshift slices, because color gradient strength varies with redshift (Suess et al. 2019a, 2019b).

At all redshifts, there is a clear relation between color gradient strength and inferred age. A Spearman correlation test indicates that this trend is statistically significant in the two lower-redshift intervals; flatter color gradients and larger error bars on individual galaxies likely contribute to the larger p-value in the highest-redshift bin. We fit this color gradient-age relation with LEO-Py, including systematic errors on inferred ages and intrinsic scatter around the relation (Feldmann 2019). We find that young quiescent galaxies have nearly flat color gradients. This result agrees with Maltby et al. (2018), who found that the optical and near-infrared sizes of post-starburst galaxies are similar. Galaxies with older stellar ages have increasingly more negative color gradients, with redder centers and/or bluer outskirts. The slope of the best-fit relation is consistent across redshift, while the normalization decreases toward lower redshift (consistent with Suess et al. 2019a).

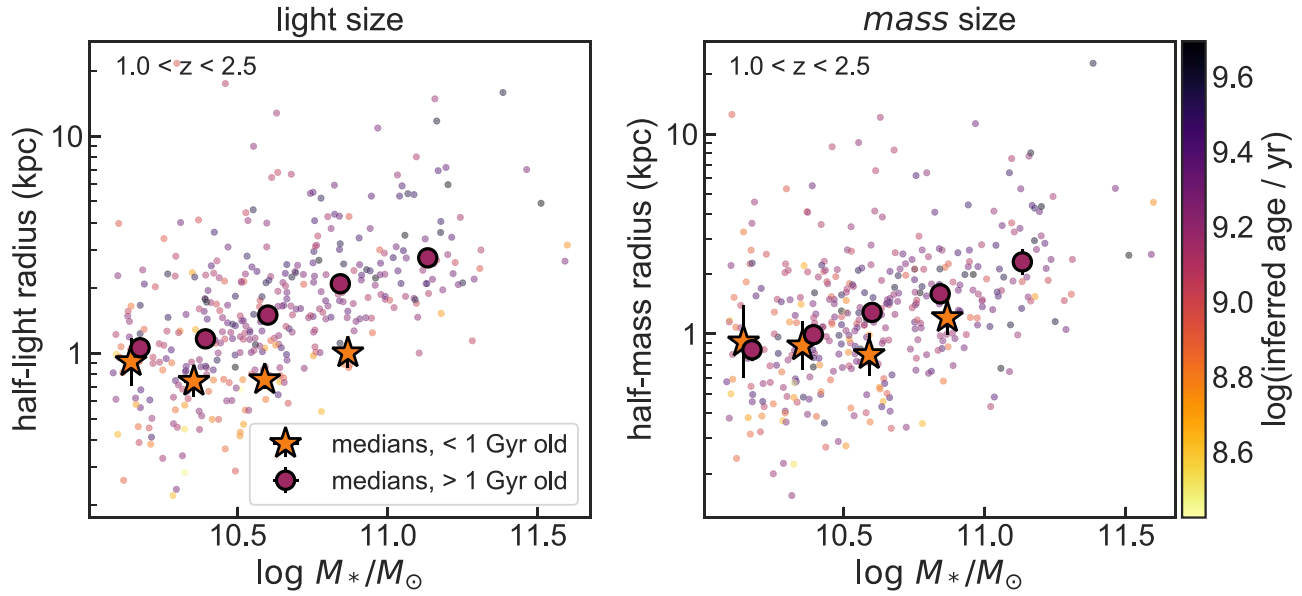

Figure 2. Half-light (left panel) and half-mass (right panel) radius as a function of stellar mass for quiescent galaxies at $1.0 \leqslant z \leqslant 2.5$. Points represent individual galaxies, colored by inferred age. Large purple circles and yellow stars show medians for old (age >1 Gyr) and young (age $\leqslant$1 Gyr) quiescent galaxies; medians are only shown for bins with $\geqslant$5 galaxies. While there is a 0.3 dex difference in the median half-light radii of young and old quiescent galaxies, this difference is reduced to only $\sim$0.1 dex when considering half-mass radii.

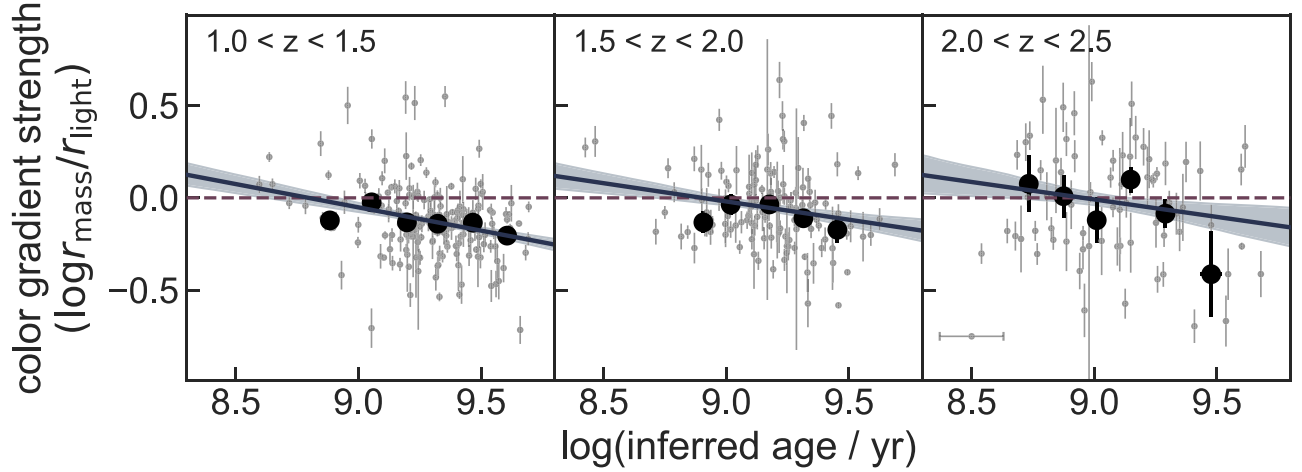

Figure 3. Color gradient strength as a function of inferred age for quiescent galaxies ($M_* \geqslant 10^{10.1} M_\odot$) in three redshift bins. Small gray points represent individual galaxies, black circles are median age bins, and the blue line and shaded region show a best-fit linear relation (and 1σ confidence interval, determined by bootstrap resampling) to the individual points. Typical uncertainties in inferred ages are shown by the error bar in the lower left of the right panel. The dashed purple line denotes no color gradient; values above (below) this line indicate bluer (redder) centers. There is a clear trend between color gradient strength and age, such that older galaxies have stronger color gradients. The slope of the relation is consistent across redshift. Spearman's ρ (p-values) for each redshift interval are -0.26 (<0.001), -0.20 (0.02), and -0.14 (0.25).

Because color gradients tend to be stronger in more massive galaxies (e.g., Tortora et al. 2010; Suess et al. 2019a) and the older galaxies in our sample have higher median stellar masses, we test whether the trend between color gradient strength and galaxy age is a reflection of the color gradient–mass relation. The trend that we see in Figure 3 persists in mass-matched subsamples, with a consistent slope; this indicates there is a relation between color gradient and age even at fixed mass. We also test whether there is a correlation between residuals in the color gradient–mass relation and residuals in the age–mass relation (e.g., Salim et al. 2015; Sanders et al. 2018). We find that there is a statistically significant trend between the two sets of residuals at all redshifts, further emphasizing that the trend between color gradient strength and age we see in Figure 3 is not purely a mass effect.

Together, Figures 2 and 3 indicate that the observed difference between the half-light radii of young and old quiescent galaxies is *not* a true difference in their sizes: instead, it is a systematic difference in their color gradients. Older quiescent galaxies have negative color gradients, making them appear larger than they truly are; meanwhile, young quiescent galaxies have flat color gradients, and appear their "true" size. This systematic difference in color gradient strength results in older quiescent galaxies *appearing* larger than post-starburst galaxies, even though their half-mass radii differ by at most $\sim$0.1 dex.

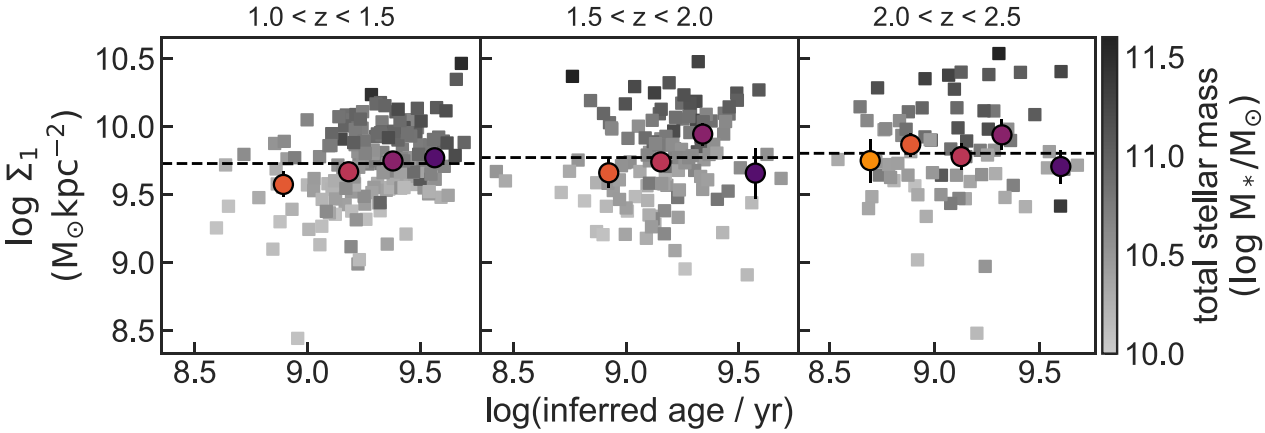

Figure 4. Mass density in the central kiloparsec of the galaxy, Σ_1, as a function of inferred age in three redshift bins. Squares show individual galaxies, shaded by total stellar mass; colored circles represent median bins in age. The dashed black line shows the median Σ_1 of all galaxies in a given redshift bin. While Σ_1 depends on total stellar mass (especially evident in the lowest-redshift bin), it varies only slightly with redshift, and does not depend on stellar age. This supports the idea that galaxies quench with consistently high Σ_1.

4. Central Densities of Quiescent Galaxies as a Function of Age

We now turn to the mass profiles of galaxies along the quiescent sequence. Previous studies have found that quiescent galaxies have consistently high central mass densities, implying that the build-up of a dense central core is a prerequisite for quenching (e.g., Cheung et al. 2012; Fang et al. 2013; van Dokkum et al. 2014; Tacchella et al. 2015; Barro et al. 2017; Mosleh et al. 2017; Whitaker et al. 2017). We calculate the central mass surface density, $\Sigma_1 \equiv M_{*,r<1\,\mathrm{kpc}}/\pi$, from the Suess et al. (2019a) mass profiles. In Figure 4 we show Σ_1 as a function of inferred age.

While the central mass densities of quiescent galaxies clearly depend on total stellar mass, at fixed mass Σ_1 is remarkably consistent across age and redshift. We find a best-fit relation[4] of

$$\begin{aligned}\log\Sigma_1 \;=\; & (9.40 \pm 0.06) + (0.69 \pm 0.03)(\log M_*/M_\odot - 10.5) \\ & +(0.78 \pm 0.17)\log(1+z) \\ & +(-0.03 \pm 0.04)(\log(\mathrm{age\ yr^{-1}}) - 9.5).\end{aligned} \quad (1)$$

Previous studies have found a dependence of $\Sigma_1 \propto (M_*/M_\odot)^{0.64}$ (Fang et al. 2013; Barro et al. 2017; Saracco et al. 2017; Tacchella et al. 2017), consistent with our fit within 1σ error bars. Both Barro et al. (2017) and Mosleh et al. (2017) calculated slightly shallower redshift evolution, $\Sigma_1 \propto (1+z)^{0.55-0.68}$, but again the values are consistent within 1σ errors. We note that the redshift evolution we find is still relatively slow, and indicates that Σ_1 decreases by only $\sim$0.13 dex between our highest and lowest redshift bin.

We find that the dependence of Σ_1 on galaxy age is consistent with zero (Equation (1), Figure 4). This implies that more compact galaxies do *not* quench earlier: in that case, older galaxies at fixed mass would have higher Σ_1. We note that the most massive galaxies quench first (e.g., Cowie et al. 1996), and more massive galaxies tend to have higher Σ_1. This effect fully accounts for the slight trend of increasing Σ_1 in older and more massive galaxies in our $1.0 \leqslant z \leqslant 1.5$ bin, and suggests that the results of Saracco et al. (2017)—who found that older and more massive galaxies have higher Σ_1—are driven by mass, not age, effects.

While we find that Σ_1 depends on stellar mass and redshift but not age, Estrada-Carpenter et al. (2020) find that Σ_1 depends on stellar mass and formation redshift. These two interpretations are not inconsistent: Σ_1 is highest in massive galaxies that form early in the universe, but does not appear to evolve as galaxies age after quenching.

Tacchella et al. (2017) found that older galaxies at fixed mass have higher Σ_1, inconsistent with our results. However, their study was performed at $z = 0.05$: this discrepancy may reflect differences in quenching mechanisms or the properties of recently quenched galaxies at $z > 1$ and $z \sim 0$ (e.g., Maltby et al. 2018).

5. Discussion

In this Letter we investigate the half-mass radii, color gradients, and central mass densities of $1.0 \leqslant z \leqslant 2.5$ quiescent galaxies as a function of age. We find that post-starburst galaxies are *not* significantly smaller than older quiescent galaxies of the same stellar mass; they only appear smaller because they have systematically flatter color gradients (Figures 2 and 3). At the same time, we see that post-starburst galaxies are compact, with central mass densities consistent with those of older quiescent galaxies of the same mass (Figure 4).

These observations can help address two separate questions: what mechanism caused post-starburst galaxies to stop forming stars? And how do quiescent galaxies evolve after they quench? To place our observations in context, Figure 5 shows the median mass profiles, color gradients, and half-mass radii of all quiescent galaxies in our sample, binned by age. Each binned point includes galaxies across our full mass and redshift range. We bin across redshift because neither half-mass radii nor Σ_1 evolve significantly over our $1.0 \leqslant z \leqslant 2.5$ range (Equation (1); Suess et al. 2019b). However, we note that the older quiescent galaxies in our sample are also more massive; therefore, each age bin probes a different stellar mass. This is

[4] This least-squares fit was performed using the python `lmfit` package for consistency with Fang et al. (2013) and Barro et al. (2017) in order to facilitate a direct comparison of the results. A LEO-Py fit including systematic error bars on the independent variables as well as intrinsic scatter around the relation finds a slightly steeper mass dependence and slightly shallower redshift dependence, consistent with the `lmfit` results within 1.5σ.

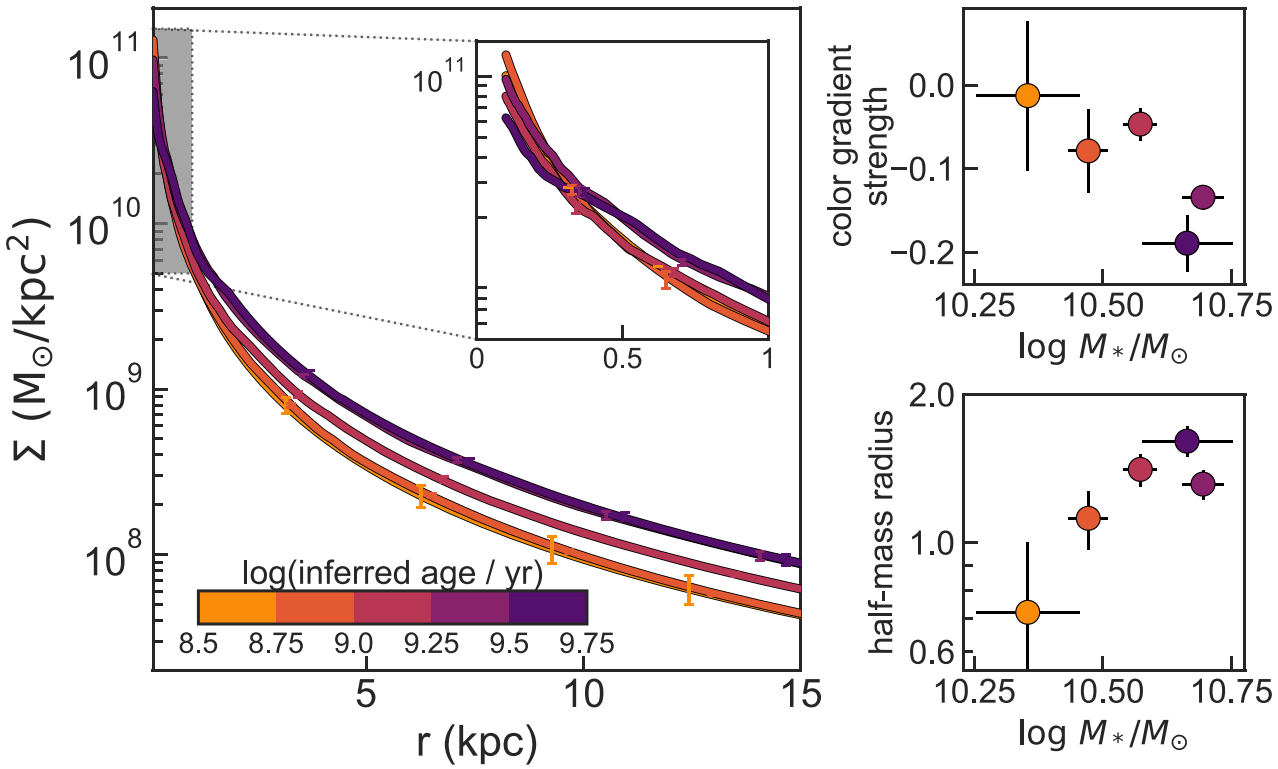

Figure 5. Left panel: mass profiles of quiescent galaxies ($1.0 \leqslant z \leqslant 2.5$) split into age bins. The central mass profiles are similar across age; extra mass in older galaxies is deposited mostly in the wings. Right panels: median color gradient strength ($\log r_{\rm mass}/r_{\rm light}$, top-right panel) and half-mass–radius (bottom-right panel) as a function of median stellar mass for the same age bins. Color gradients are flatter in younger galaxies; the older galaxies in our sample are also generally more massive (and thus larger).

not simply selection bias: our sample is complete to the same mass limit in each redshift bin (Figure 1).

First, we consider how post-starburst galaxies halt their star formation. If slow or gradual processes such as gas exhaustion are responsible, we would expect the sizes, structures, and color gradients of post-starburst galaxies to resemble those of their progenitors. However, we see in Figures 3 and 5 that post-starburst galaxies have flat color gradients, while Suess et al. (2019a) found that star-forming galaxies at similar masses and redshifts typically have negative color gradients. Because color gradients indicate radial variations in the underlying stellar populations, in order to alter the color gradients in a galaxy some physical process must either create new stellar populations or re-arrange existing ones. Candidate processes include mergers—which could flatten or destroy radial color gradients—or a central starburst, which could create an excess of young stars at the center of the galaxy and flatten a pre-existing negative color gradient. Both of these processes are popular candidates for the fast quenching process, whereby galaxies rapidly build a massive core before shutting off their star formation (e.g., Tacchella et al. 2015; Zolotov et al. 2015; Barro et al. 2017; Woo & Ellison 2019).

Second, we turn to the question of how galaxies evolve after they quench. In Figures 3 and 5 we see that older and more massive galaxies also have stronger negative color gradients; this indicates that some process must re-establish negative color gradients after quenching. At the same time, we see that the shapes of their mass profiles change (left panel, Figure 5) and their half-mass radii grow (bottom-right panel, Figure 5). Older quiescent galaxies have slightly less centrally peaked mass profiles, potentially due to post-quenching adiabatic expansion (e.g., Choi et al. 2018) or dynamical friction from mergers (e.g., Naab et al. 2009). Older quiescent galaxies also have more mass at large radii, resulting in larger average sizes. These observations are consistent with a picture where quiescent galaxies grow "inside-out" at late times: minor mergers deposit younger and/or lower-metallicity stars at the outskirts of galaxies, causing negative radial color gradients (e.g., Bezanson et al. 2009; Naab et al. 2009; Suess et al. 2019a). In this scenario, we would expect older quiescent galaxies—which have had time for more inside-out growth—to have more negative color gradients, higher total stellar masses, more mass in their outskirts, and thus larger sizes. This is a good match for what we see in Figure 5.

This picture relies on interpreting the ages of quiescent galaxies as an evolutionary sequence. It is important to verify this assumption and ensure that our results are not driven by selection effects. One possibility is that the trends we see are caused by evolution in the properties of recently quenched galaxies ("progenitor bias," e.g., Carollo et al. 2013; Poggianti et al. 2013). In the Lilly & Carollo (2016) model, star-forming galaxies have negative color gradients, which strengthen as galaxies grow; these color gradients cease to evolve after quenching. In a pure progenitor bias scenario, older quiescent galaxies formed earlier and should thus have flatter color gradients, because star-forming galaxies at higher redshift have flatter color gradients (Suess et al. 2019a, 2019b). However, we see that older quiescent galaxies actually have *steeper* color gradients (Figure 3). This model is thus inconsistent with our observations. Furthermore, while quiescent galaxies at high redshift have flat or even positive color gradients, old quiescent galaxies at low redshift have negative color gradients

(Figure 3). This also implies that color gradients evolve after quenching, inconsistent with the Lilly & Carollo (2016) model. Finally, the observed evolution of half-mass radii at $1.0 \leqslant z \leqslant 2.5$ can be almost entirely explained by minor mergers alone, without the need for progenitor bias (Suess et al. 2019b).

A second possibility is that not all quiescent galaxies go through a post-starburst phase, so not all of the progenitors of old quiescent galaxies are included in our sample. Indeed, the number densities of post-starburst galaxies are not sufficiently high to explain the full growth of the quiescent sequence at these redshifts (e.g., Wild et al. 2016; Belli et al. 2019). Recent work has suggested that green valley galaxies—which lie just outside of our *UVJ* selection—may represent a second, slower, path to join the quiescent sequence (e.g., Bremer et al. 2018; Wu et al. 2018; Belli et al. 2019; Woo & Ellison 2019). If green valley galaxies quench without significantly altering their structural properties (Wu et al. 2018), we would expect them to have negative color gradients inherited from their star-forming progenitors. The trend we see between color gradient strength and age could thus be explained without appealing to post-quenching evolution *if* all old quiescent galaxies with negative color gradients quenched via the green valley, and all old quiescent galaxies with flat color gradients quenched via the post-starburst route. However, the presence of old quiescent galaxies with negative color gradients in our highest-redshift bin—where quenching through the green valley is less prevalent (e.g., Belli et al. 2019)—indicates that this selection effect does not fully account for the trends we see in this Letter. We will investigate the color gradients and half-mass radii of green valley galaxies in detail in a forthcoming paper.

Altogether, our observations appear consistent with a picture where post-starburst galaxies quench after experiencing a rapid core-building process; after quenching, we observe changes in the quiescent population that appear consistent with inside-out growth via minor mergers. This work was enabled by studying radial color gradients and their evolution directly: not only are color gradients a valuable observable in their own right, they are essential for obtaining an unbiased view of galaxy size evolution. In the future, when upcoming missions such as James Webb Space Telescope provide spatially resolved information through the infrared, we hope that this work will spur future investigations into color gradients as a powerful probe of galaxy evolution.

K.A.S. thanks Sirio Belli, Vince Estrada-Carpenter, and Sandro Tacchella for inspiring discussions and helpful comments. We also thank the anonymous referee whose suggestions improved this Letter. This work is funded by grant AR-12847, provided by NASA though a grant from the Space Telescope Science Institute (STScI) and by NASA grant NNX14AR86G. This material is based upon work supported by the National Science Foundation Graduate Research Fellowship Program under grant No. DGE 1106400.

ORCID iDs

Katherine A. Suess https://orcid.org/0000-0002-1714-1905
Mariska Kriek https://orcid.org/0000-0002-7613-9872
Sedona H. Price https://orcid.org/0000-0002-0108-4176
Guillermo Barro https://orcid.org/0000-0001-6813-875X

References

Almaini, O., Wild, V., Maltby, D. T., et al. 2017, MNRAS, 472, 1401
Barro, G., Faber, S. M., Koo, D. C., et al. 2017, ApJ, 840, 47
Barro, G., Kriek, M., Pérez-González, P. G., et al. 2016, ApJL, 827, L32
Belli, S., Newman, A. B., & Ellis, R. S. 2015, ApJ, 799, 206
Belli, S., Newman, A. B., & Ellis, R. S. 2019, ApJ, 874, 17
Bezanson, R., van Dokkum, P. G., Tal, T., et al. 2009, ApJ, 697, 1290
Bremer, M. N., Phillipps, S., Kelvin, L. S., et al. 2018, MNRAS, 476, 12
Carollo, C. M., Bschorr, T. J., Renzini, A., et al. 2013, ApJ, 773, 112
Chabrier, G. 2003, PASP, 115, 763
Cheung, E., Faber, S. M., Koo, D. C., et al. 2012, ApJ, 760, 131
Choi, E., Somerville, R. S., Ostriker, J. P., Naab, T., & Hirschmann, M. 2018, ApJ, 866, 91
Cowie, L. L., Songaila, A., Hu, E. M., & Cohen, J. G. 1996, AJ, 112, 839
Dekel, A., & Burkert, A. 2014, MNRAS, 438, 1870
Estrada-Carpenter, V., Papovich, C., Momcheva, I., et al. 2020, ApJ, 898, 171
Fang, J. J., Faber, S. M., Koo, D. C., & Dekel, A. 2013, ApJ, 776, 63
Feldmann, R. 2019, A&C, 29, 100331
Greene, J. E., Janish, R., Ma, C.-P., et al. 2015, ApJ, 807, 11
Grogin, N. A., Kocevski, D. D., Faber, S. M., et al. 2011, ApJS, 197, 35
Hopkins, P. F., Bundy, K., Murray, N., et al. 2009, MNRAS, 398, 898
Koekemoer, A. M., Faber, S. M., Ferguson, H. C., et al. 2011, ApJS, 197, 36
Lee, B., Giavalisco, M., Whitaker, K., et al. 2018, ApJ, 853, 131
Lilly, S. J., & Carollo, C. M. 2016, ApJ, 833, 1
Maltby, D. T., Almaini, O., Wild, V., et al. 2018, MNRAS, 480, 381
Mosleh, M., Tacchella, S., Renzini, A., et al. 2017, ApJ, 837, 2
Naab, T., Johansson, P. H., & Ostriker, J. P. 2009, ApJL, 699, L178
Poggianti, B. M., Moretti, A., Calvi, R., et al. 2013, ApJ, 777, 125
Salim, S., Lee, J. C., Davé, R., & Dickinson, M. 2015, ApJ, 808, 25
Sanders, R. L., Shapley, A. E., Kriek, M., et al. 2018, ApJ, 858, 99
Saracco, P., Gargiulo, A., Ciocca, F., & Marchesini, D. 2017, A&A, 597, A122
Straatman, C. M. S., Spitler, L. R., Quadri, R. F., et al. 2016, ApJ, 830, 51
Suess, K. A., Kriek, M., Price, S. H., & Barro, G. 2019a, ApJ, 877, 103
Suess, K. A., Kriek, M., Price, S. H., & Barro, G. 2019b, ApJL, 885, L22
Tacchella, S., Carollo, C. M., Faber, S. M., et al. 2017, ApJL, 844, L1
Tacchella, S., Carollo, C. M., Renzini, A., et al. 2015, Sci, 348, 314
Tacchella, S., Dekel, A., Carollo, C. M., et al. 2016, MNRAS, 458, 242
Tortora, C., Napolitano, N. R., Cardone, V. F., et al. 2010, MNRAS, 407, 144
van de Sande, J., Kriek, M., Franx, M., et al. 2013, ApJ, 771, 85
van der Wel, A., Franx, M., van Dokkum, P. G., et al. 2014, ApJ, 788, 28
van Dokkum, P. G., Bezanson, R., van der Wel, A., et al. 2014, ApJ, 791, 45
van Dokkum, P. G., Nelson, E. J., Franx, M., et al. 2015, ApJ, 813, 23
Whitaker, K. E., Bezanson, R., van Dokkum, P. G., et al. 2017, ApJ, 838, 19
Whitaker, K. E., Kriek, M., van Dokkum, P. G., et al. 2012, ApJ, 745, 179
Wild, V., Almaini, O., Dunlop, J., et al. 2016, MNRAS, 463, 832
Wild, V., Taj Aldeen, L., Carnall, A., et al. 2020, MNRAS, 494, 529
Woo, J., & Ellison, S. L. 2019, MNRAS, 487, 1927
Wu, P.-F., van der Wel, A., Bezanson, R., et al. 2018, ApJ, 868, 37
Wu, P.-F., van der Wel, A., Bezanson, R., et al. 2020, ApJ, 888, 77
Yano, M., Kriek, M., van der Wel, A., & Whitaker, K. E. 2016, ApJL, 817, L21
Zolotov, A., Dekel, A., Mandelker, N., et al. 2015, MNRAS, 450, 2327